Image Reconstruction from Nonuniformly-spaced Samples in Fourier Domain Optical Coherence Tomography

Jun Ke, Rui Zhu, Edmund Y. Lam

Imaging Systems Laboratory, Department of Electrical and Electronic Engineering, University of Hong Kong, Pokfulam, Hong Kong

ABSTRACT

In this work, we use inverse imaging for object reconstruction from nonuniformly-spaced samples in Fourier domain optical coherence tomography (FD-OCT). We first model the FD-OCT system with a linear system of equations, where the source power spectrum and the nonuniformly-spaced sample positions are represented accurately. Then, we reconstruct the object signal directly from the nonuniformly-spaced wavelength measurements. With the inverse imaging method, we directly estimate the 2D cross-sectional object image instead of a set of independent A-line signals. By using the Total Variation (TV) as a constraint in the optimization process, we reduce the noise in the 2D object estimation. Besides TV, object sparsity is also used as a regularization for the signal reconstruction in FD-OCT. Experimental results demonstrate the advantages of our method, as we compare it with other methods.

Keywords: Fourier domain optical coherence tomography (FD-OCT), inverse imaging, nonuniform discrete Fourier transform (NUDFT), L_1 norm, total variation (TV)

1. INTRODUCTION

Fourier domain optical coherence tomography (FD-OCT) is a technology to image a sample's internal structure in a depth range of several millimeters with an axial resolution smaller than $10\,\mu$m.[1–5] Conventionally the image of the internal structure is reconstructed by taking fast Fourier transform (FFT) of system measurement samples. Fourier transformation requires the samples are uniformly spaced in wavenumber domain, while FD-OCT measurements are collected uniformly in wavelength domain. The nonlinear correspondence between wavelength and wavenumber hence causes a nonuniformly sampling issue in FD-OCT.[6] In the conventional FFT method, an interpolation method is used to preprocess system measurements before the transformation. Although multiple kinds of interpolation methods have been studied, such measurement preprocessing strategy still faces challenges such as improving system sensitivity roll-off in axial direction, increasing system local signal-to-noise ratio (SNR), and suppressing side-lobe artifacts.[7,8]

Recently nonuniform discrete Fourier transform (NUDFT) is studied to avoid this resampling precess.[7–9] NUDFT is defined as the Fourier transform and the inverse Fourier transform of a nonuniformly sampled signal.[10,11] The transformation result can also be uniformly or nonuniformly spaced. With NUDFT, the reconstructed signal in FD-OCT presents better performance such as less sensitivity roll-off at deeper positions.[8] However, note that both the FFT and the NUDFT methods are based on an assumption that the signal reconstruction is a Fourier transformation of system measurements. In this paper, we use inverse imaging method[12,13] to solve the reconstruction problem. By using a right regularization according to the signal's prior knowledge, we expect inverse imaging presents better reconstruction compared with the two Fourier transformation methods.

The paper is organized as follows. In Section 2, we first model FD-OCT measurement using a linear equation system. Then two inverse imaging methods, the L_0-norm regularization method[14] and the total variation (TV) regularization method,[15,16] are studied for signal reconstruction. In Section 3, experiment results used FFT, NUDFT, the L_0-norm regularization, and the TV-norm regularization are compared. In Section 4, we draw the conclusions for the work.

Further author information: (Send correspondence to Edmund Lam)
Edmund Lam: E-mail: elam@eee.hku.hk

Computational Imaging X, edited by Charles A. Bouman, Ilya Pollak, Patrick J. Wolfe, Proc. of SPIE-IS&T Electronic Imaging, SPIE Vol. 8296, 829610
 · doi: 10.1117/12.907331

2. FOURIER DOMAIN OPTICAL COHERENCE TOMOGRAPHY (FD-OCT)

There are two kinds of FD-OCT systems, spectral-domain OCT (SD-OCT) and swept-source OCT (SS-OCT). Although SD-OCT and SS-OCT have differences such as the system source, the detection device, and the measurement collecting speed, both system measurement processes can be modeled using the same equation. In this work, we use SD-OCT as an example to study the nonuniformly sampling issue in FD-OCT.

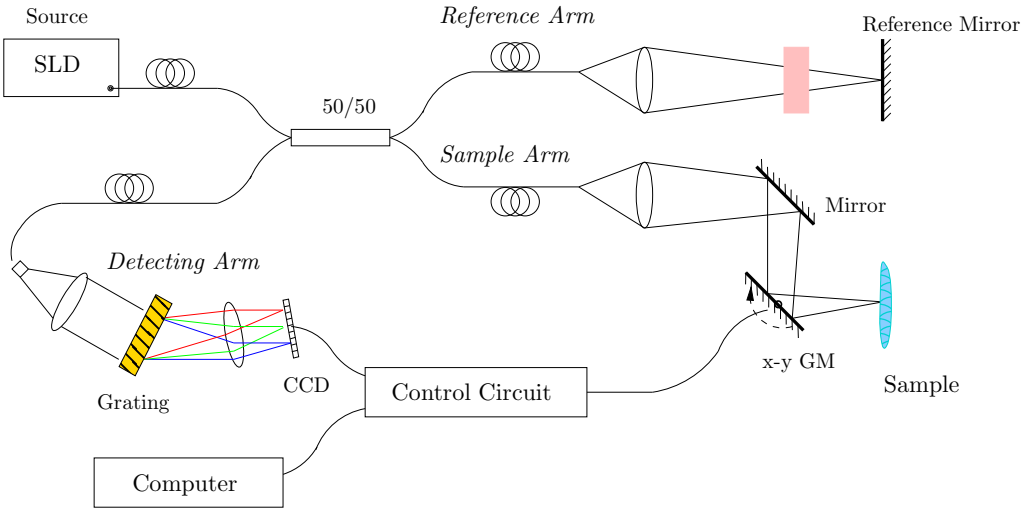

Figure 1. The SD-OCT system diagram.

Figure 1 presents a SD-OCT system diagram. In such a system, the output is the interference between the reflected light from the reference mirror and the sample. System measurements for an A-line in FD-OCT can be represented as[6]

$$I(k) = G(k)\left\{p_r^2 + 2\int_0^\infty p_r p_s(z)\cos(2a_s kz)\,\mathrm{d}z + \iint_0^\infty p_s(z)p_s(z')\mathrm{e}^{\mathrm{j}2ka_s(z-z')}\,\mathrm{d}z\,\mathrm{d}z'\right\}. \quad (1)$$

In this equation, $k = 2\pi/\lambda$ is the wavenumber corresponding to the wavelength λ, $I(k)$ is the system measurement, $G(k)$ is the source power spectrum, p_r is the reflective ratio of the reference mirror, $p_s(z)$ is the reflective ratio of the sample at a depth value z, and a_s is the sample refractive index assumed to be 1 in this work. To reconstruct the sample signal $p_s(z)$ from the measurement $I(k)$, the conventional method is to calculate the FFT of $I(k)$. This method has advantages such as fast computation speed and easy to implementation. However, as discussed in the introduction section, the first issue the method encountered is the nonuniformly spaced samples in the discrete measurement domain. As shown in Figure 1, the interference signal after the 50/50 coupler enters the system detecting arm, which is consisted of a customized spectrometer. In the spectrometer, the interference signal is dispersed by a grating, then detected by a line detector array, CCD. Because the light after the grating is dispersed uniformly according to wavelength, the data measured by CCD are uniformly distributed in λ-domain, hence nonuniformly in k-domain. This causes less samples are collected in the larger k value region. To reconstruct the sample signal from such nonuniformly spaced measurements, the linear or cubic interpolation has been used in the FFT method. NUDFT has also been studied and implemented into FD-OCT. Here we will discuss another strategy for the reconstruction problem.

Before continuing the discussion, we simplify the measurement model in Equation (1) first. The reflective ratio of the reference mirror p_r is assumed as 1. The source power spectrum $G(k)$ is estimated and subtracted from $I(k)$. The estimation of $G(k)$ will be discussed in the next section. Because the third term in Equation (1) is smaller compared with the other two, we represent it as an error. Then the FD-OCT measurement can be

written as

$$I(k_m) = 2G(k_m) \sum_{n=0}^{N-1} p_s(z_n) \cos(2k_m z_n) + e(k_m), \tag{2}$$

where $m \in \{0, 1, \ldots, M-1\}$ denotes the mth pixel of the CCD camera, and $e(k_m)$ is the measurement error at wavenumber k_m. Equation (2) can also be written into a matrix formulation. We use a vector of size $(M \times 1)$, $\mathbf{y} = [I(k_0) \;\; I(k_1) \;\; \cdots \;\; I(k_{M-1})]^T$, to represent the measurements. A matrix H denotes the projection matrix of size $(M \times N)$, where the (m, n)th element is

$$\mathsf{H}_{m,n} = 2G(k_m) \cos(2k_m z_n)$$

and $n \in \{0, 1, \ldots, N-1\}$. The sample signal for one A-line is represented by a vector of size $(N \times 1)$, $\mathbf{x} = [p_s(z_0) \;\; p_s(z_1) \;\; \cdots \;\; p_s(z_{N-1})]^T$. The measurement error vector is defined as $\mathbf{e} = [e(k_0) \;\; e(k_1) \;\; \cdots \;\; e(k_{M-1})]^T$. Then, with these notifications the matrix formulated measurement process becomes

$$\mathbf{y} = \mathsf{H}\mathbf{x} + \mathbf{e}. \tag{3}$$

For a 2D sample cross-sectional image consisted of L A-lines, the measurement model becomes

$$\mathsf{Y} = \mathsf{H}\mathsf{X} + \mathsf{E}, \tag{4}$$

where matrixes $\mathsf{Y}(M \times L)$, $\mathsf{X}(N \times L)$, and $\mathsf{E}(M \times L)$ represent the L A-line measurement vectors, the 2D sample signal, and the error vectors, respectively. To reconstruct the sample signal back based on the projection matrix H and using system measurements is an inverse problem. As described earlier, two inverse imaging methods, the L_0-norm method and the TV method, are used.

In the L_0-norm method, the object is assumed sparse in a domain, such as the spatial domain or the wavelet transformation domain. Such an assumption has been used fairly common in a signal reconstruction problem.[14,17,18] In this work, we assume the signal is sparse in the wavelet transformation domain. We use a vector θ of size $(N \times 1)$ and a matrix W of size $(N \times N)$ to represent the sparse wavelet coefficients and the wavelet transformation, respectively. Then the sample vector $\mathbf{x}$ can be represented as $\mathbf{x} = \mathsf{W}\theta$. To use the L_0-norm method for signal reconstruction, the following optimization method is solved,[14]

$$\theta_{\text{est}} = \min_{\theta} \;\; \|\mathbf{y} - \mathsf{H}\mathsf{W}\theta\|^2 + \frac{2\log(2)\log(N)}{\epsilon}\|\theta\|_0, \tag{5}$$

where ϵ is a parameter directly related to the norms of the signal $\mathbf{x}$ and the error vector $\mathbf{e}$, or the signal-to-noise ratio in system measurement. Note that, the cost function in this minimization problem includes two parts, one for the error in measurement domain and the other for the sparsity L_0-norm regularization. The solution to the problem is a minimizer θ_{est} which has $\mathsf{H}\mathbf{x}_{\text{est}} = \mathsf{H}\mathsf{W}\theta_{\text{est}}$ close to the measurement $\mathbf{y}$ and is also sparse in the wavelet transformation domain. The following two-step iterative algorithm[14] is used to solve this optimization problem,

1. $\varphi^{(t)} = \theta^{(t)} + \alpha(\mathsf{H}\mathsf{W})^{\mathrm{T}}(\mathbf{y} - \mathsf{H}\mathsf{W}\theta^{(t)})$

2. $\theta_i^{(t+1)} = \begin{cases} \varphi_i^{(t)} & \text{if } \; |\varphi_i^{(t)}| \geq \delta_0 \\ 0 & \text{otherwise} \end{cases}$,

where t is the iteration index, the positive parameters α and δ_0 are the update step size and the threshold used to constraint signal's sparsity.

The second inverse imaging method is the TV method. In such a method, the 2D sample signal X is estimated directly by solving following minimization problem,[19]

$$\mathsf{X}_{\min} = \min_{\mathsf{X}} \;\; ||\mathsf{H}\mathsf{X} - \mathsf{Y}||_2^2 + \beta||\mathsf{X}||_{TV} \tag{6}$$

where $\beta > 0$ is a penalty parameter, $||\mathsf{X}||_{TV}$ is the total variation of the sample signal matrix X,

$$\|\mathsf{X}\|_{TV} = \sum_{1 \le n \le N, 1 \le l \le L} \sqrt{|(\nabla X)^x_{n,l})|^2 + |(\nabla X)^y_{n,l})|^2}$$

with

$$(\nabla X)^x_{n,l} = \begin{cases} X_{n+1,l} - X_{n,l} & \text{if } n < N \\ 0 & \text{if } n = N \end{cases}, \quad (\nabla X)^y_{n,l} = \begin{cases} X_{n,l+1} - U_{n,l} & \text{if } l < L \\ 0 & \text{if } l = L \end{cases}.$$

Same as in the L_0-norm method, the cost function defined in Equation (6) includes two parts, one for the error in the measurement domain and the other for the sample matrix TV norm value, respectively. By balancing the two parts, the solution of the problem has $\mathsf{HX}_{\min}$ agree with the system measurements Y and also has a small noise residue in the term of a small 2D variation value. Multiple approaches are available to solve this problem. We choose a fast TV method as presented in Figure 2. In this method, an additional intermediate matrix U is used. The algorithm to solve this new defined optimization problem is also a two-step iterative process, which is defined in Figure 2 too. The first step can be considered as a deconvolution process for an unconstrained signal reconstruction problem. The second[20] is to denoise the signal reconstruction result from step 1 using the TV regularization.

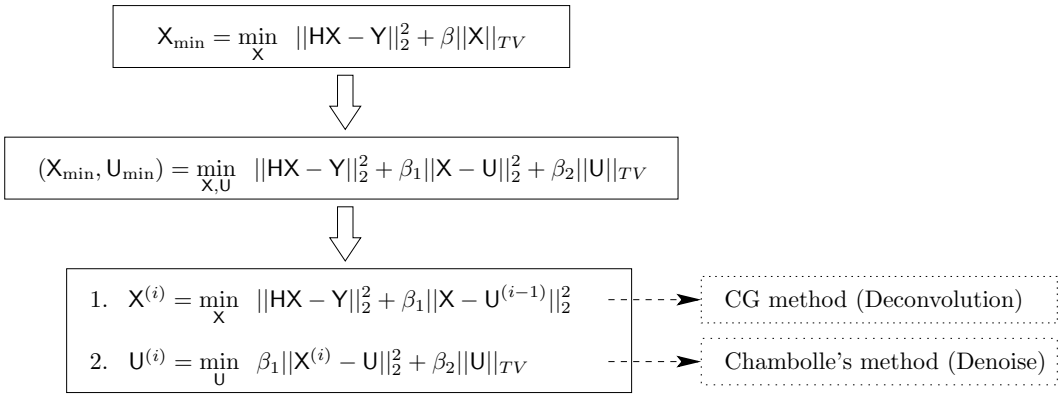

Figure 2. The TV method.[19, 20]

3. EXPERIMENT RESULT

The experiment set-up in this work uses a Super-Luminescent Diode (SLD) source with a center wavelength at 840nm and a bandwidth of 40nm. The system depth resolution in air is 7.78 μm. The maximal detectable depth is 3mm. The reference mirror is a silver coated mirror with 2 inch diameter. The customized spectrometer is consisted of an Edmund Optics 1 inch VPH grating and a line scan camera. We use a computer to control the CCD camera and the x-y scan Galvona mirror GM. Using this set-up, 1000 A-lines with 2048 measurements per A-line for a cross-sectional image of a pear are collected.

As described in last section, the source spectrum $G(k_m)$ is estimated before reconstructing the signal. Figure 3 (a) presents the raw measurements for 10 out of 1000 A-lines. It can observed that there is a slow varying signal in the raw measurement. This signal is the source specturm $G(k_m)$. A rectangular shape low-pass filter in the Fourier transform domain is used to extract this signal from the raw measurement of an A-line. Then we average such filtered signals over all 1000 A-lines to reduce the residue error in the estimation. Figure 3 (b) presents the final estimated $G_{\text{est}}(k_m)$. Subtracting $G_{\text{est}}(k_m)$ from system raw measurements, we have the measurements as shown in Figure 3 (c). These measurements can be written into a linear equation system as defined in Equation (3) and (4).

Four methods are used to reconstruct the sample signal. The first is the conventional FFT method where the measurements for each A-line is resampled before the fast Fourier transform. The cubic interpolation method is

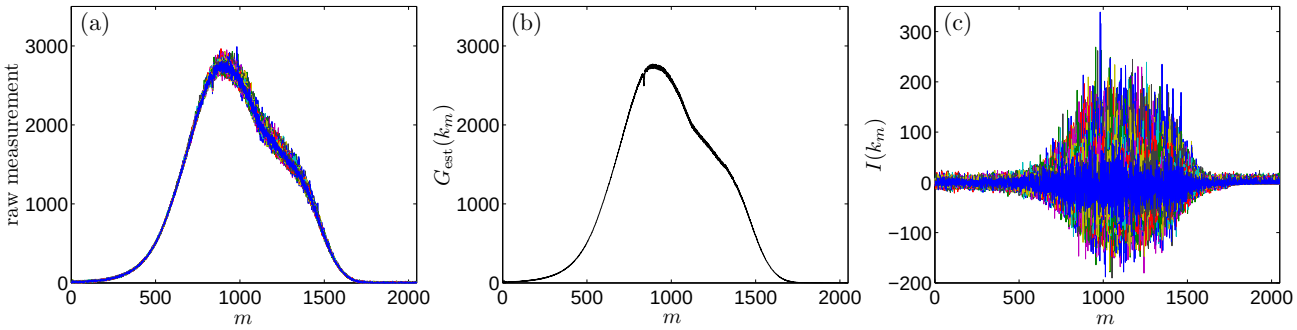

Figure 3. (a) 10 A-line raw measurements; (b) the estimated source power spectrum $G_{\text{est}}(k_m)$, and (c) $I(k_m)$ after subtracting $G_{\text{est}}(k_m)$ from raw measurements.

used for the resampling process. The second is the NUDFT method, which has a slower computation speed but generates more accurate result compared with the FFT method. The third method is the L_0-norm method. The last one is the TV method as defined in Equation (6). Note that, in the first three methods, the sample signal in each A-line is reconstructed independently, while in the TV method, the 2D signal X is reconstructed directly from the nonuniformly spaced measurements Y.

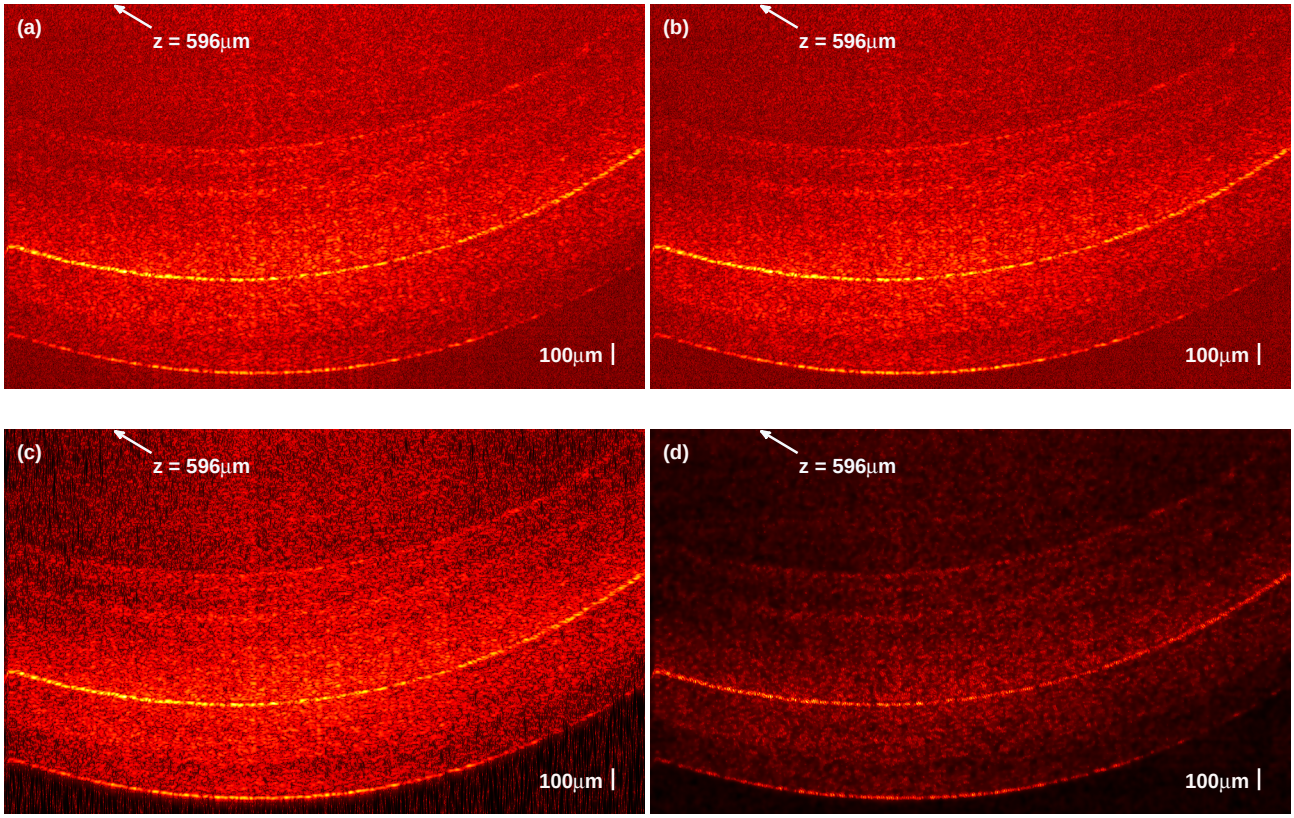

Figure 4. Reconstructed cross-sectional sample signals using (a) the FFT, (b) the NUDFT, (c) the L_0-norm, and (d) the TV methods.

The cross-sectional sample reconstructions using the four methods are presented in Figure 4. Zoomed-in parts of the four reconstructions and the reconstructions for the A-line $L = 300$ are presented in Figure 5 and

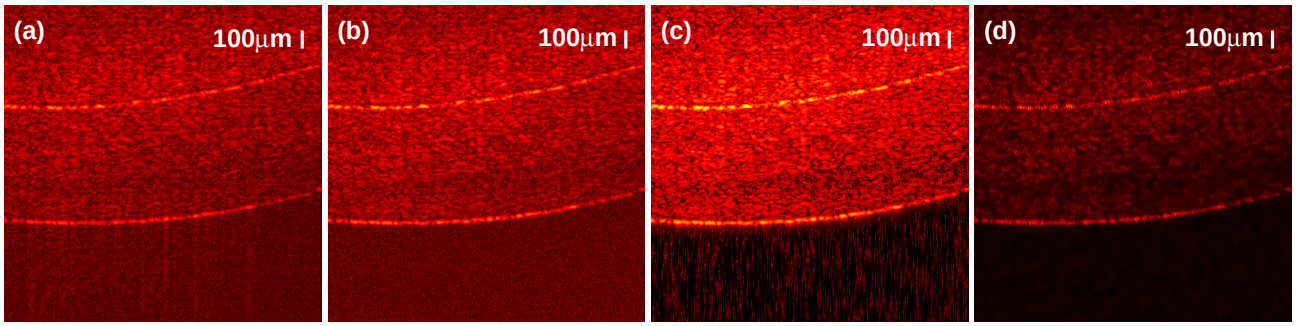

Figure 5. Zoomed in cross-sectional sample signal reconstructions using (a) the FFT, (b) the NUDFT, (c) the L_0-norm, and (d) the TV methods.

6, respectively. Comparing these results, it can be observed that the reconstruction using the NUDFT method presents better performance compared with the conventional FFT method, especially at a large depth z_n value. This is cohesive with other people's observation.[7–9] However, among the forth methods, the reconstruction using the TV method presents the least noise residue, hence with the best signal-to-noise ratio. Between the two inverse imaging methods, the L_0-norm method eliminates some small reconstructed sample values. However, overall it is hard to claim its performance is better than the NUDFT method. Therefore, the TV value is a powerful regularization for reducing noise and enhancing edge.

4. CONCLUSION

In this work, we model the FD-OCT system with a linear equation system and discuss the inverse imaging methods with the L_0-norm regularization and the TV regularization for signal reconstruction. The reconstructions using FFT and NUDFT methods are also presented and compared with the results obtained using both inverse imaging methods. Using the TV regularization, a 2D cross-sectional sample signal can be estimated directly from FD-OCT system nonuniformly spaced samples. Among the four methods, the reconstruction using the TV method presents the smallest noise residue and the best signal-to-noise contrast compared with the other three.

Acknowledgment

This work was supported in part by the University Research Committee of the University of Hong Kong under Project 10208648.

REFERENCES

[1] Drexler, W. and Fujimoto, J. G., [*Optical Coherence Tomography Technology and Applications*], Springer-Verlag Berlin Heidelberg (2008).

[2] Drexler, W., "Ultrahigh-resolution optical coherence tomography," *Journal of Biomedical Optics* **9**(1), 47–74 (2004).

[3] Huang, D., Swanson, E. A., Lin, C. P., Schuman, J. S., Stinson, W. G., Chang, W., Hee, M. R., Flotte, T., Gregory, K., Puliafito, C. A., and Fujimoto, J. G., "Optical coherence tomography," *Science* **254**(5035), 1178–1181 (1991).

[4] Cheng, K. H. Y., Standish, B. A., Yang, V. X. D., Cheung, K. K. Y., Gu, X., Lam, E. Y., and Wong, K. K. Y., "Wavelength-swept spectral and pulse shaping utilizing hybrid fourier domain modelocking by fiber optical parametric and erbium-doped fiber amplifiers," *Optics Express* **18**(3), 1909–1915 (2010).

[5] Zhu, R., Xu, J., Zhang, C., Chan, A. C., Li, Q., Chui, P. C., Lam, E. Y., and Wong, K. K., "Dual-band time-multiplexing swept-source OCT based on optical parametric amplification," *IEEE Journal of Selected Topics in Quantum Electronics* (2011). Accepted.

[6] Brezinski, M., [*Optical Coherence Tomography-Principles and Applications*], Elsevier Inc. (2006).

[7] Zhang, K. and Kang, J. U., "Graphic processing unit accelerated non-uniform fast Fourier transform for ultrahigh-speed, real-time Fourier-domain OCT," *Optics Express* **18**(22), 23472–23487 (2010).

[8] Wang, K., Ding, Z., Wu, T., Wang, C., Meng, J., Chen, M., and Xu, L., "Development of a non-uniform discrete Fourier transform based high speed spectral domain optical coherence tomography system," *Optics Express* **17**(14), 12121–12131 (2009).

[9] Chan, H. K. and Tang, S., "High-speed spectral domain optical coherence tomography using non-uniform fast Fourier transform," *Biomedical Optics Express* **1**(5), 1309–1319 (2010).

[10] Rudin, L. I., Osher, S., and Fatemi, E., "An accurate algorithm for nonuniform fast Fourier transforms (NUFFT's)," *IEEE Microwave and guided wave letters* **8**(1), 18–20 (1998).

[11] Greengard, L. and Lee, J.-Y., "Accelerating the nonuniform fast Fourier transform," *SIAM Review* **46**(3), 443–454 (2004).

[12] Ke, J., Poon, T. C., and Lam, E. Y., "Depth resolution enhancement in optical scanning holography with a dual-wavelength laser source," *Applied Optics* **50**, H285–H296 (December 2011).

[13] Lam, E. Y., Zhang, X., Vo, H., Poon, T. C., and Indebetouw, G., "Three-dimensional microscopy and sectional image reconstruction using optical scanning holography," *Applied Optics* **48**, H113–H119 (December 2009).

[14] Haupt, J. and Nowak, R., "Signal reconstruction from noisy random projections," *IEEE Transactions on Information Theory* **52**(9), 4036–4048 (2006).

[15] Rudin, L. I., Osher, S., and Fatemi, E., "Nonlinear total variation based noise removal algorithms," *Physica D: Nonlinear Phenomena* **60**(1-4), 259–268 (1992).

[16] Ke, J., Zhu, R., and Lam, E. Y., "Image reconstruction from nonuniform samples in spectral domain optical coherence tomography," in [*OSA Topic Meeting in Signal Recovery and Synthesis*], SMD2, OSA (2011).

[17] Needell, D. and Tropp, J., "Cosamp: Iterative signal recovery from incomplete and inaccurate samples," *Applied and Computational Harmonic Analysis* **26**(3), 301–321 (2009).

[18] Gilbert, A. and Tropp, J., "Signal recovery from random measurements via orthogonal matching pursuit," *IEEE Transactions on Information Theory* **53**(12), 4655–4666 (2007).

[19] Huang, Y., Ng, M. K., and Wen, Y., "A fast total variation minimization method for image restoration," *Multiscale Modeling & Simulation* **7**(2), 774–795 (2008).

[20] Chambolle, A., "An algorithm for total variation minimization and applications," *Journal of Mathematical Imaging and Vision* **20**, 89–97 (2004).

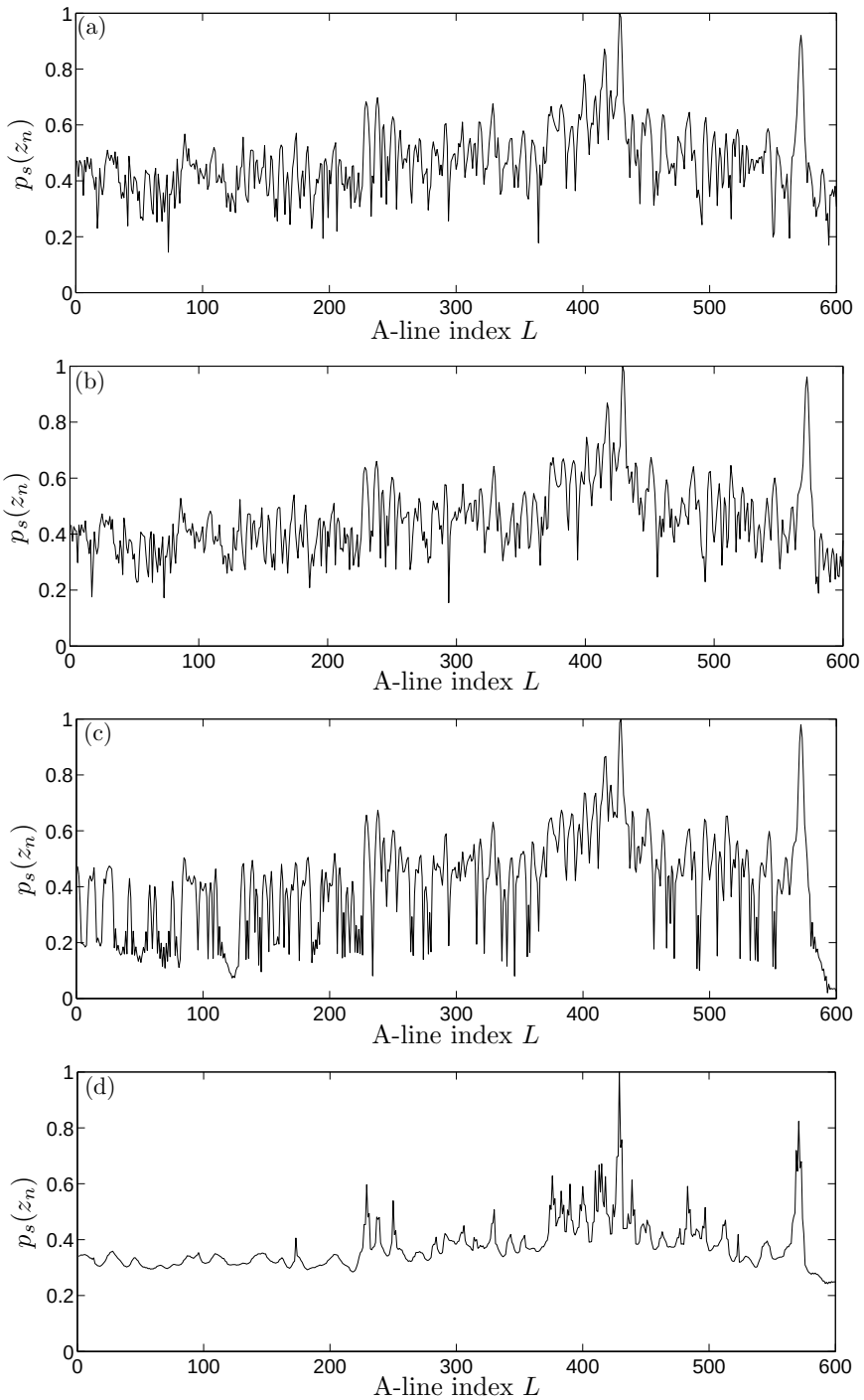

Figure 6. Reconstruction for A-line $L = 300$ using (a) the FFT, (b) the NUDFT, (c) the L_0-norm, and (d) the TV methods.